Progress In Electromagnetics Research C, Vol. 74, 181–189, 2017

Circular Slotted Elliptical Patch Antenna with Elliptical Notch in Ground

Bhupendra K. Shukla*, Nitesh Kashyap, and Rajendra K. Baghel

Abstract—A circular slotted elliptical patch antenna with an elliptical notch in ground for L-band and S-band application is presented. The proposed antenna consists of an elliptical patch with a circular notch on the top layer of a substrate, and a wide elliptical slot and an elliptical notch with two symmetrical slots on the bottom layer of the same substrate. The proposed antenna was fabricated on an FR-4 substrate ($\tan(\delta)$= 0.02,ε_r= 4.3) with the thickness of 1.6 mm, and it was excited by coaxial feed joined with microstrip line through via. The proposed antenna exhibited the bandwidth of 102.58% from 1.32 GHz to 4.1 Hz for $|S_{11}| < -10$ dB. Surface current distribution and radiation pattern at resonating frequencies 1.71, 2.28, 3.03 and 3.84 GHz were analyzed. Evolution of the antenna and effect of parameters were also studied to know the behavior of the antenna.

1. INTRODUCTION

Printed slot antennas are becoming popular in modern wireless communication due to their attractive features such as cheap manufacturing, small volume, reasonable gain, easy integration with microwave circuitry and active devices [1]. The limitation of a narrow slot antenna is narrow impedance bandwidth [2]. This limitation is eliminated by using wide slot and multi-slot antennas. Slots produce new edges of the fringing fields and alter the resonance frequency of the fundamental mode (TM_{10} or TM_{01}) and other higher order mode (TM_{12}, TM_{20}) or generate new resonance frequency near fundamental mode [3–5]. Wide slot antennas offer a large number of resonating modes, and using proper tuning element these modes are overlapped and broadband operations realized [6]. The impedance bandwidth of a wide-slot antenna depends on the shape of the slot and the feed line structure. Some reported wide-slot shapes are triangular [7], rectangular [8], rhombus [9], elliptical [10], U [11], hexagonal [12] and octagonal [13]. The shape of the patch also alters mutual coupling and impedance matching of the antenna. In [14], A-shaped antenna was proposed that covered a bandwidth from 2.9 GHz to 11.5 GHz. Some other reported shapes of the patch with wide slot are circle [15] square [16] and deformed hexagon [17]. In this communication, we present a circularly slotted elliptical patch antenna with an elliptical notch in ground for L-band and S-band application, and the proposed antenna is investigated numerically and experimentally. Initially, the elliptical notch and circular notch are incorporated on the ground and patch, respectively. Further, two symmetrical slots are placed on corners of the ground plane to enhance the performance of the antenna. The proposed antenna covers the bandwidth of 102.58% from 1.32 GHz to 4.1 Hz. This antenna shows a bidirectional pattern in E-plane and omnidirectional pattern in H-plane. In addition, simulated current distributions with the evolution of antenna are also discussed, and the parametric study is carried out to observe the behavior of the antenna.

Received 27 March 2017, Accepted 26 May 2017, Scheduled 2 June 2017
* Corresponding author: Bhupendra Kumar Shukla (bhupendrashuklaphd@gmail.com).
The authors are with the Maulana Azad National Institute of Technology, Bhopal, India.

2. ANTENNA GEOMETRY

Geometry and dimension of the proposed antenna are displayed in Figure 1. The proposed structure is placed on x-y plane and symmetric about a longitudinal axis. Elliptical patch (R_{p1} (semi-major axis radius) and R_{p2} (semi-minor axis)) with a circular notch (R_{p3}) and 50 Ω microstrip line (M_{pl} (length of feed line) and M_{wp} (width of feed line)) are printed on the top layer of a fiberglass polymer resin (FR4) substrate with a thickness (h) = 1.6 mm, dielectric constant (ε_r) = 4.3, and loss tangent ($\tan\delta$) = 0.02. On the bottom side of the substrate, one elliptical wide slot (R_{g3}) with the eccentricity of 0.97 and another elliptical notch (R_{g1} (semi-minor axis) R_{g2} (semi-major axis radius)) are incorporated. Elliptical notch on the ground plane is the key element that improves the impedance matching of the antenna. Further two symmetrical parasitic slots (L_{g1} and W_{g1}) are employed on the corners of the ground plane. The proposed structure is energized by coaxial feed connected with a microstrip line through via. The overall volume of the antenna is $(70 \times 50 \times 1.6)\,\text{mm}^3$. Optimized dimensions of proposed antenna are listed in Table 1.

Table 1. Parameters and their dimension.

Parameter	Dimension	Parameter	Dimension
M_{wp}	3 mm	M_{lp}	16.5 mm
R_{g1}	4.6 mm	R_{g3}	24 mm
R_{g2}	10 mm	L_g	70 mm
R_{p1}	18 mm	W_g	50 mm
R_{p2}	14.66 mm	R_{p3}	10.66 mm
L_{g1}	11.45 mm	W_{g1}	10.56 mm

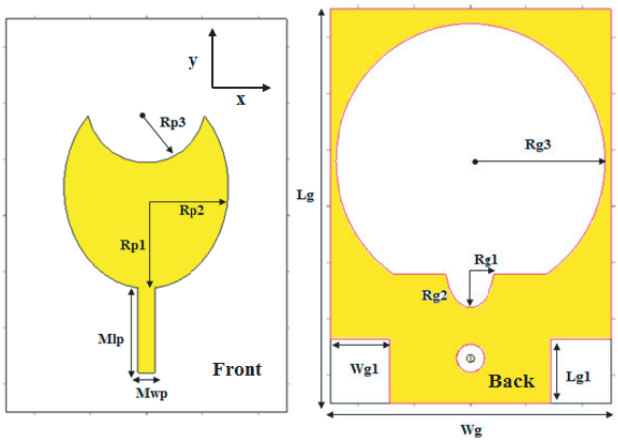

Figure 1. The geometry of proposed antenna.

Figure 2. Fabricated proposed antenna.

3. RESULT AND DISCUSSION

A prototype of proposed antenna is depicted in Figure 2. Figure 3 exhibits the comparison between measured and simulated return losses against frequency. Initially, the reflection coefficient of the proposed antenna is investigated numerically from 1 GHz to 6 GHz, and further return loss is measured using VNA (vector network analyzer). The proposed antenna covers the bandwidth of 102.58% from 1.32 GHz to 4.1 GHz for $|S_{11}| < -10$ dB. The other resonating band is observed from 5.58 GHz to 6 GHz. A small error of 6.91% is found between simulated (1.266 GHz) and measured (1.32 GHz) lower cutoff

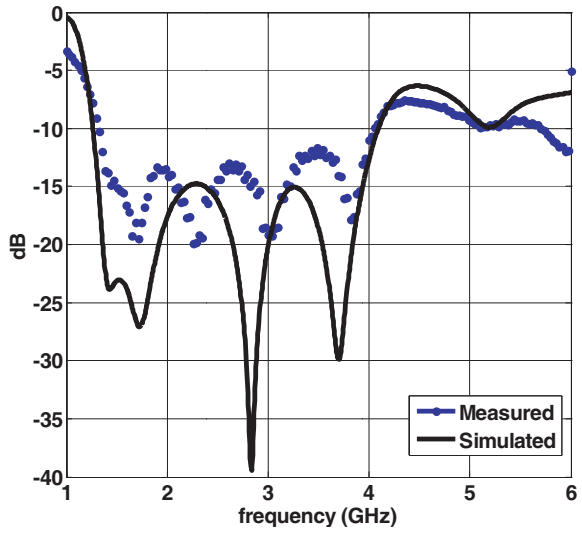

Figure 3. Comparison of measured and simulated return loss against frequency.

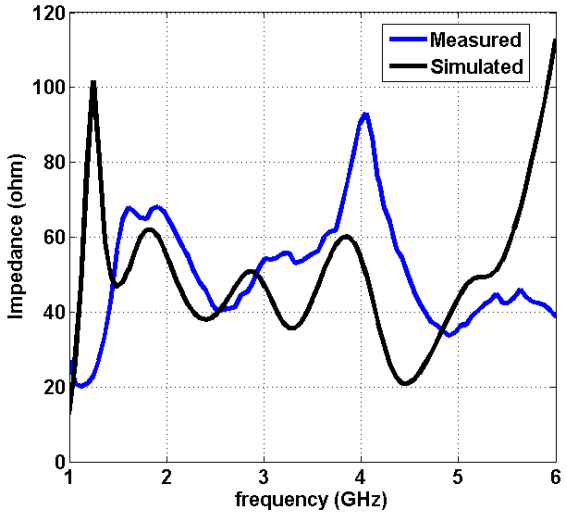

Figure 4. Comparison of simulated and measured real part of the input impedance.

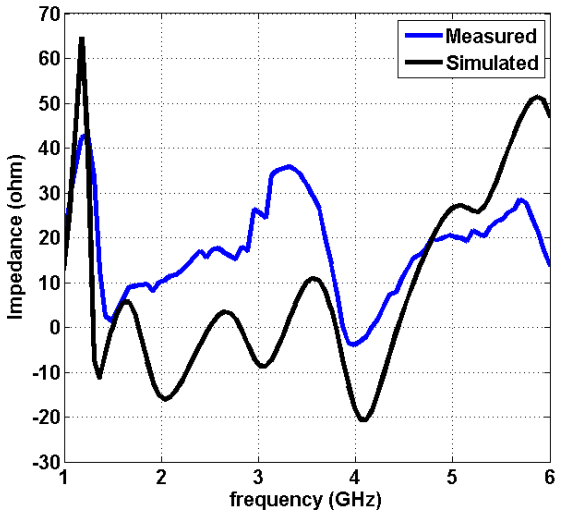

Figure 5. Comparison of simulated and measured imaginary part of the input impedance.

frequencies. The difference between simulated and measured return losses is because of fabrication error, SMA connector, and ground plane effect.

Comparison between real (simulated and measured) parts of the input impedance is illustrated in Figure 4. It is clear from the figure that real (measured) part varies between $36\,\Omega$ and $90\,\Omega$ in the entire frequency band. A variation of the imaginary part of the input impedance is depicted in Figure 5. Simulated imaginary part oscillates around $0\,\Omega$ while measured imaginary part varies between $35\,\Omega$ and $-5\,\Omega$.

The difference between measured and simulated impedances (Figures 4 and 5) is due to ground plane effect losses through connector and fabrication error. The current distributions at lower cutoff frequency and resonating frequencies are displayed in Figure 6. It is exhibited from the figure that the lower cutoff frequency is generated because of edges of the ground plane. Lower cutoff frequency f_l is calculated by following equations.

$$L_o = L_1 + L_2 + L_3 + L_4 \tag{1}$$

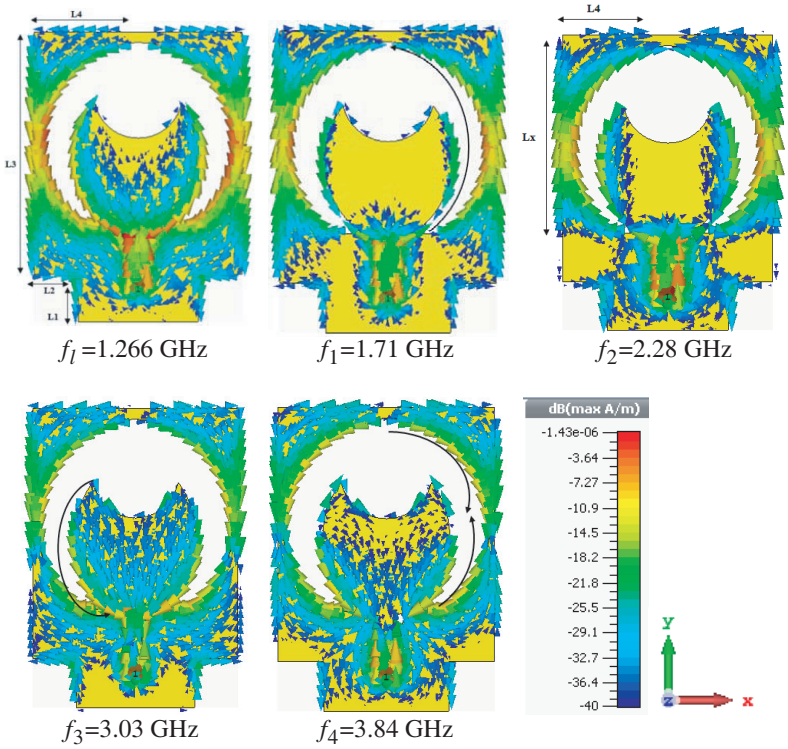

Figure 6. Surface current distribution at the lower cut-off frequency and resonating frequencies.

$$f_l = \frac{C}{L_o\sqrt{\varepsilon_r}} \tag{2}$$

where L_o is distance shown in Figure 6. Calculated, simulated and measured lower cutoff frequencies are 1.35 GHz, 1.266 GHz and 1.32 GHz, respectively. A small error of 2.22% between calculated and measured lower cutoff frequency is found. At fundamental frequency $f_1 = 1.71$ GHz, one half wave variation of the current vectors is found along the wide slot. The fundamental frequency is produced by wide slot, and this frequency is calculated by the resonance frequency equation of circular patch [18].

$$a_{eff} = a\left[1 + \frac{2h}{\pi\varepsilon_r a}\left\{\ln\left(\frac{a}{2h}\right) + (1.7726)\right\}\right]^{1/2} \tag{3}$$

$$f_1 = \frac{1.8412v_0}{2a_{eff}\pi\sqrt{\varepsilon_r}} \tag{4}$$

where a is the radius of circular wide slot, h the thickness of substrate, a_{eff} the effective radius, v_0 the speed of light, and ε_r the permittivity the substrate. At the second resonating frequency, current pattern along the edge of the ground plane is changed, and this frequency is calculated by the following equation.

$$L_{f_2} = L_x + L_4 \tag{5}$$

$$f_2 = \frac{c}{L_{f_2}\sqrt{\varepsilon_r}} \tag{6}$$

The third resonating frequency is produced by an elliptical patch. At this frequency, one half variation of current is found along the elliptical patch, and resonating frequency f_3 is calculated by given equations [19].

$$a_{eff} = a\left[1 + \frac{2h}{\pi\varepsilon_r a}\left\{\ln\left(\frac{a}{2h}\right) + (1.41\varepsilon_r + 1.77)\frac{h}{a}(0.268\varepsilon_r + 1.65)\right\}\right]^{1/2} \tag{7}$$

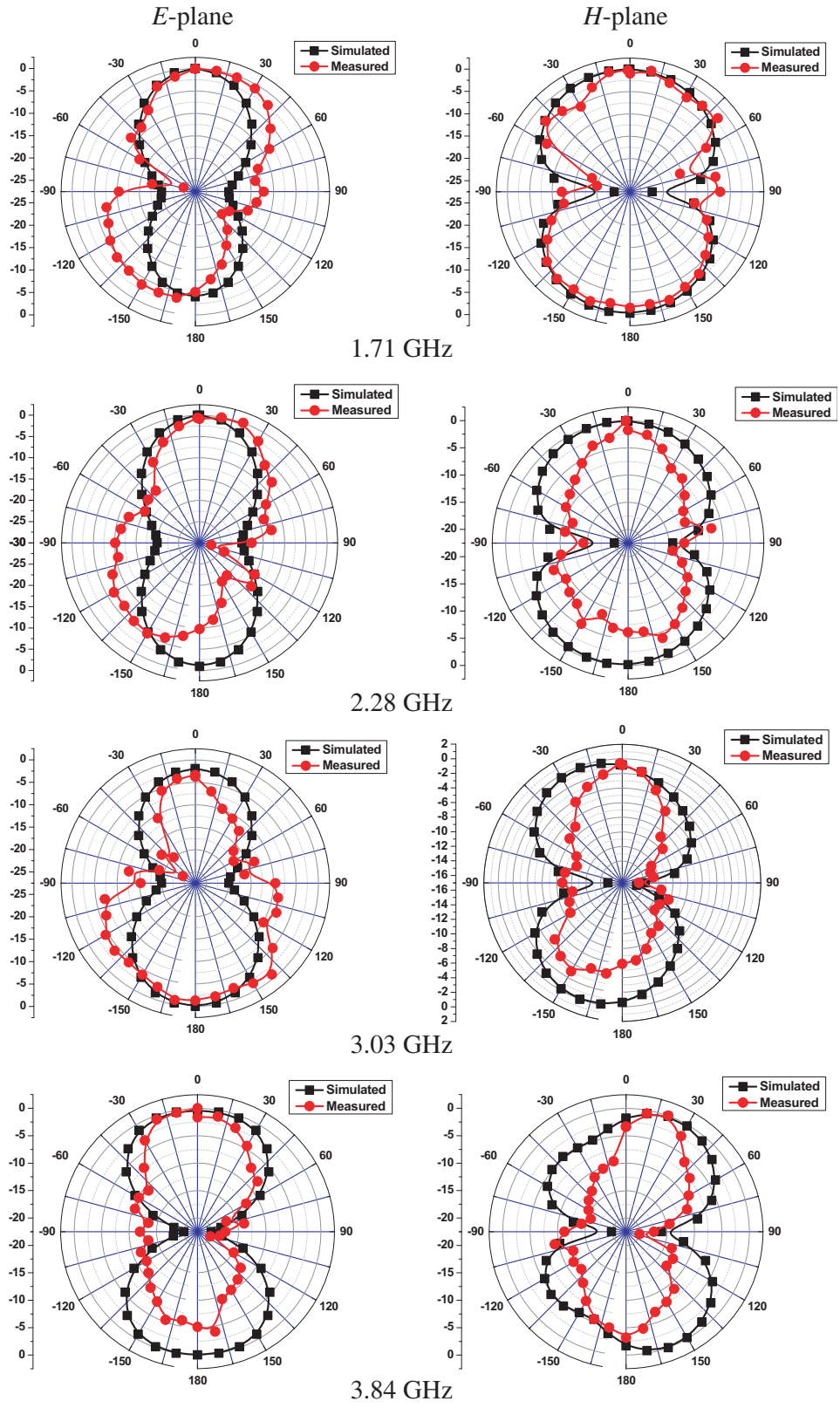

Figure 7. Far field pattern at resonating frequencies.

$$f_{11}^{e,o} = \frac{15}{\pi e a_{eff}} \sqrt{\frac{q_{11}^{e,o}}{\varepsilon_r}} \tag{8}$$

$$q_{11}^{e} = -0.0049e + 3.7888e^2 - 0.7278e^3 + 2.314e^4 \tag{9}$$

$$q_{11}^{o} = -0.0063e + 3.8316e^2 - 1.1351e^3 + 5.2229e^4 \tag{10}$$

At the fourth resonating frequency, two half-wave variations of current along the wide slot are found. The fourth resonating frequency is the second harmonic of the fundamental frequency. It is also observed that current patterns are symmetrical about the y-axis. The radiation patterns of the proposed antenna at resonating frequencies 1.71, 2.28, 3.03 and 3.84 GHz are depicted in Figure 7. At E-plane, bidirectional pattern is found. Measured results in E-plane differ from simulated ones because of radiation from coaxial cable at lower frequencies and fabrication error. In H plane, omni and quasi-omnidirectional patterns are found at all resonating frequencies. Omni-directionality is lost in frequency 3.84 GHz because of higher order modes. Table 2 exhibits the value of simulated and measured gains and simulated radiation efficiency at resonating frequencies.

Table 2. Gain and radiation efficiency.

Frequency (GHz)	Simulated gain (dB)	Measured gain (dB)	Simulated radiation efficiency
1.71	2.85	2.80	0.97
2.28	2.98	3.95	0.974
3.03	4.04	4.81	0.955
3.84	4.73	5.52	0.92

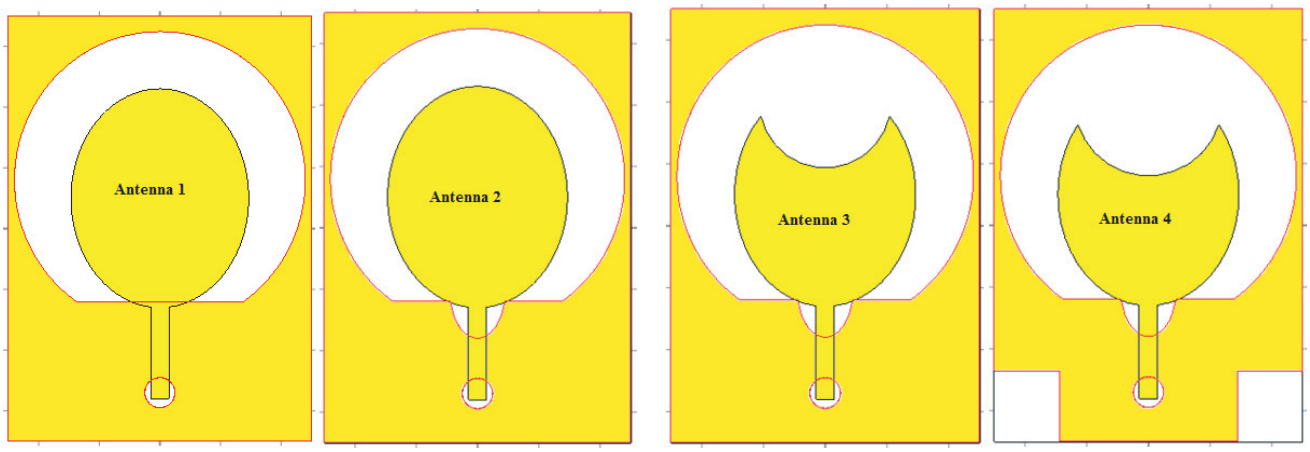

Figure 8. Evolution of antenna.

4. EVOLUTION OF ANTENNA AND PARAMETRIC STUDY

Comparison of frequency responses of antenna 1, antenna 2, antenna 3 and antenna 4 is shown in Figure 9. Antenna 1 resonates in two frequency bands, and to improve the bandwidth of antenna 1, elliptical notch is incorporated on the periphery of the wide slot. This notch performs two functions, i.e., introducing capacitive effect and tuning of modes. Further, one circular notch is employed on the patch. This circular notch improves the performance of antenna 2. In addition, two symmetrical slots are created to lower VSWR and increase the return loss in the resonating band. Antenna 3 and antenna

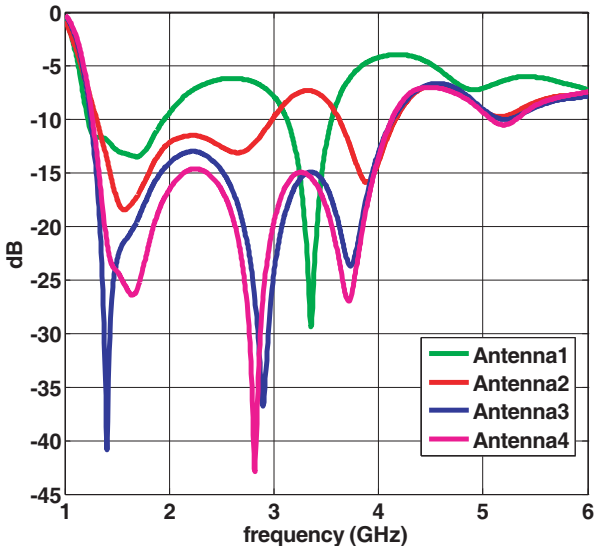

Figure 9. Comparison of return loss.

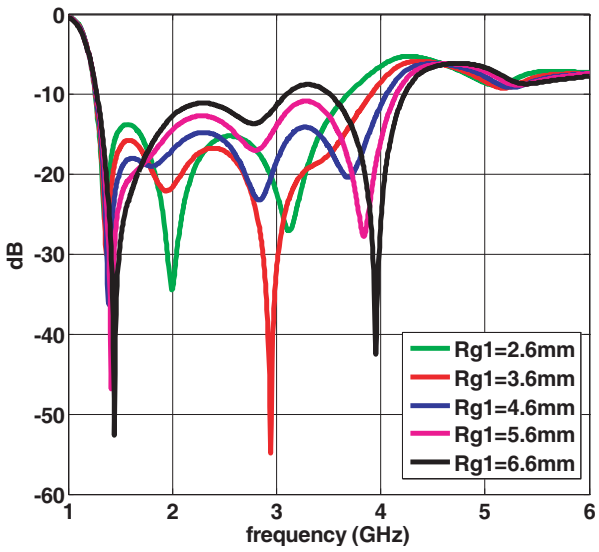

Figure 10. The impact of R_{g1} on proposed antenna.

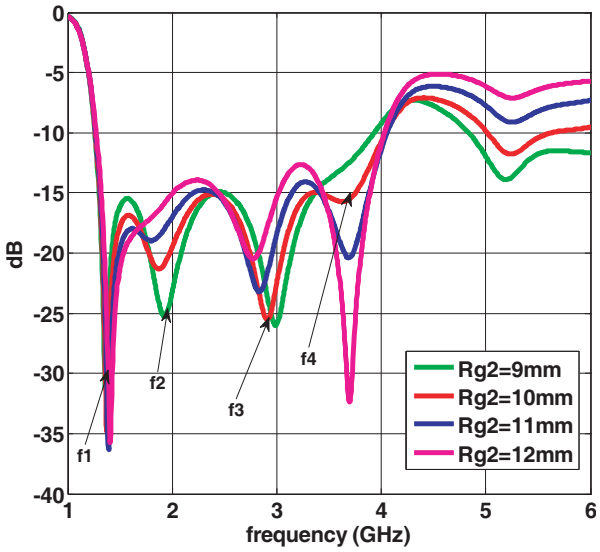

Figure 11. The impact of R_{g2} on proposed antenna.

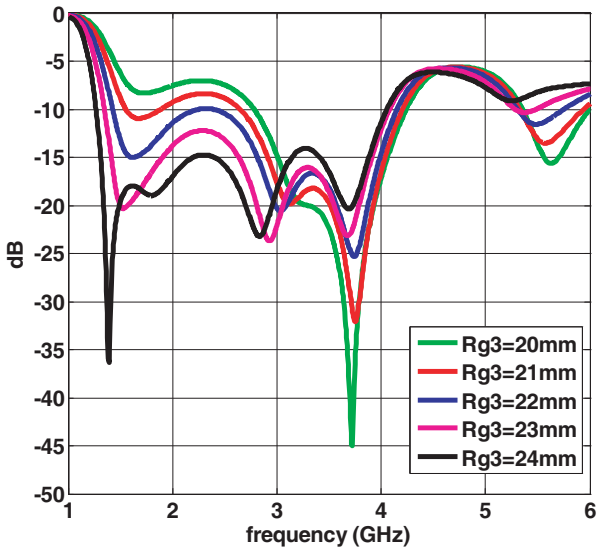

Figure 12. The impact of R_{g3} on proposed antenna.

4 show the same bandwidth of 107.35%. Evolution of the antenna is shown in Figure 8. Initially, an elliptical patch with a partial wide elliptical slot on the ground plane is employed. Further, to improve the bandwidth of antenna one elliptical notch is embedded on the periphery of the wide slot. In addition, one circular notch is created on the periphery of the patch. Finally, two symmetrical parasitic slots are incorporated on the corner of the ground plane. The impact of R_{g1} on return loss characteristics of the proposed antenna is shown in Figure 10. R_{g1} is altered from 2.6 mm to 6.6 mm. Higher cutoff frequency and first resonating frequency are shifted right with increasing the limit of R_{g1}. Maximum return loss of -52 dB is obtained for $R_{g1} = 6.6$ mm while maximum bandwidth is found for $R_{g1} = 5.6$ mm. Figure 11 exhibits the impact of R_{g2} on the frequency response of the proposed antenna.

It is clearly shown in Figure 11 that the impedance bandwidth is independent of R_{g2} while return loss is affected at different resonating frequencies. By increasing the value of R_{g2}, the first resonance

frequency f_1 deviates to the right side while second resonance frequency f_2 is moved to the left side, and it disappears at $R_{g2} = 12\,\text{mm}$. The third resonance frequency f_3 deviates to the left side, and the fourth resonating frequency f_4 is stable with increasing the value of R_{g2}. The dimension of R_{g2} is changed from 9 mm to 12 mm. Impact of R_{g3} on the frequency response of the antenna is illustrated in Figure 12. The value of R_{g3} is varied from 20 mm to 24 mm. It is clear from Figure 12 that by increasing the value of R_{g3} the impedance bandwidth of the proposed antenna is improved and return loss in enhanced in a lower frequency band.

5. CONCLUSION

A circularly slotted elliptical patch antenna with an elliptical notch in ground for L-band and S-band application is investigated. This antenna covers the bandwidth of 102.58% from 1.32 GHz to 4.1 GHz for $|S_{11}| < -10\,\text{dB}$, and it also covers the bandwidth from 5.58 GHz to 6 GHz. A small error of 6.91% is found at lower cutoff frequency (simulated and measured). The current distributions of resonating frequencies (1.71, 2.28, 3.03 and 3.84 GHz) and lower cutoff frequency are studied. Far-field pattern is omnidirectional and bidirectional at all frequencies, and the small difference is found between the simulated and measured radiation patterns. Evolution of the antenna and effect of parameters are also studied.

REFERENCES

1. Ling, L. X., T. A. Denidni, L. N. Zhang, R. H. Jin, J. P. Geng, and Q. Yu, "Printed binomial-curved slot antennas for various wideband applications," *IEEE Transactions on Microwave Theory and Techniques*, Vol. 59, No. 4, 1058–1065, April 2011.
2. Yoshimura, Y., "A microstripline slot antenna (short papers)," *IEEE Transactions on Microwave Theory and Techniques*, Vol. 20, No. 11, 760–762, November 1972.
3. Deshmukh, A. A. and K. P. Ray, "Formulation of resonance frequencies for dual-band slotted rectangular microstrip antennas," *IEEE Antennas and Propagation Magazine*, Vol. 54, No. 4, 78–97, August 2012.
4. Deshmukh, A. A. and K. P. Ray, "Analysis of broadband Psi shaped microstrip antennas," *IEEE Antennas and Propagation Magazine*, Vol. 55, No. 2, 107–123, April 2013.
5. Ansari, J. A., A. Singh, and M. Aneesh, "Desktop shaped broadband microstrip patch antenna for wireless communication," *Progress In Electromagnetics Research Letters*, Vol. 50, 13–18, 2014.
6. Tang, M. C., R. W. Ziolkowski, and S. Xiao, "Compact hyper band printed slot antenna with stable radiation properties," *IEEE Transactions on Antennas and Propagation*, Vol. 62, No. 6, 2962–2969, June 2014.
7. Chen, J. S., "Studies of CPW-fed equilateral triangular-ring slot antennas and triangular-ring slot coupled patch antennas," *IEEE Transactions on Antennas and Propagation*, Vol. 53, No. 7, 2208–2211, July 2005.
8. Yao, F. W., S. S. Zhong, W. Wang, and X. L. Liang, "Wideband slot antenna with a novel microstrip feed," *Microwave and Optical Technology Letters*, Vol. 46, No. 3, 275–278, August 2005.
9. Yea, J. J. and L. C. Wang, "Printed wideband rhombus slot antenna with a pair of parasitic strips for multiband applications," *IEEE Transactions on Antennas and Propagation*, Vol. 57, No. 4, 1267–1270, April 2009.
10. Abbosh, A. M. and M. E. Bialkowski, "Design of ultrawideband planar monopole antennas of circular and elliptical shape," *IEEE Transactions on Antennas and Propagation*, Vol. 56, No. 1, 17–23, January 2008.
11. Mandal, K. and P. P. Sarkar, "High gain wide-band U-shaped patch antennas with modified ground planes," *IEEE Transactions on Antennas and Propagation*, Vol. 61, No. 4, 2279–2282, April 2013.
12. Ghaderi, M. R. and F. Mohajeri, "A compact hexagonal wide-slot antenna with microstrip-fed monopole for UWB application," *IEEE Antennas and wireless Propagation Letters*, Vol. 10, 682–685, 2011.

13. Lui, W. J., C. H. Cheng, and H. B. Zhu, "Improved frequency notched ultrawideband slot antenna using square ring resonator," *IEEE Transactions on Antennas and Propagation*, Vol. 55, No. 9, 2445–2450, September 2007.
14. Shrivastava, M. K., A. K. Gautam, and B. K. Kanaujia, "A novel a-shaped monopole-like slot antenna for ultra wide band applications," *Microwave and Optical Technology Letters*, Vol. 56, No. 8, 1826–1829, August 2014.
15. Zhong, Y. W., G. M. Yang, and L. R. Zheng, "Planar circular patch with elliptical slot antenna for ultrawideband communication applications," *Microwave and Optical Technology Letters*, Vol. 57, No. 2, 325–328, February 2015.
16. Emadian, S. R., C. Ghobadi, J. Nourinia, M. H. Mirmozafari, and J. Pourahmadazar, "Bandwidth enhancement of CPW-fed circle-like slot antenna with dual band-notched characteristic," *IEEE Antennas and Wireless Propagation Letters*, Vol. 11, 543–546, 2012.
17. Al-Azza, A. A., F. J. Harackiewicz, and H. R. Gorla, "Very compact open-slot antenna for wireless communication systems," *Progress In Electromagnetics Research Letters*, Vol. 51, 73–78, 2015.
18. Balanis, C. A., *Aantenna Theory Analysis and Design*, John Wiley & Sons, 2005.
19. Agrawal, A., D. Vakula, and N. V. S. N. Sarma, "Design of elliptical micro strip patch antenna using ANN," *PIERS Proceedings*, 264–268, Suzhou, China, Sep. 12–16, 2011.